Superfluidity of fermions with repulsive on-site interaction in an anisotropic optical lattice near a Feshbach resonance

B Wang[1] **and L-M Duan**

FOCUS Center and MCTP, Department of Physics, University of Michigan, Ann Arbor, MI 48109, USA
E-mail: binwz@umich.edu

Abstract. We present a numerical study on ground state properties of a one-dimensional (1D) general Hubbard model (GHM) with particle-assisted tunnelling rates and repulsive on-site interaction (positive-U), which describes fermionic atoms in an anisotropic optical lattice near a wide Feshbach resonance. For our calculation, we utilize the time evolving block decimation (TEBD) algorithm, which is an extension of the density matrix renormalization group and provides a well-controlled method for 1D systems. We show that the positive-U GHM, when hole-doped from half-filling, exhibits a phase with coexistence of quasi-long-range superfluid and charge-density-wave orders. This feature is different from the property of the conventional Hubbard model with positive-U, indicating the particle-assisted tunnelling mechanism in GHM brings in qualitatively new physics.

The combination of Feshbach resonance and optical-lattice techniques has opened up possibilities for investigating strongly interacting ultracold atoms under tunable configurations [1]. Ability to control such strongly interacting systems provides an unprecedented opportunity to explore interesting states of matter. Much interesting physics has been predicted for ultracold atom systems with fundamental Hubbard model Hamiltonians. For example, with the Bose–Hubbard model and its derivations, people have studied the transition from superfluid to Mott-insulator [2], the existence of supersolid order [3], etc for ultracold bosons, whereas with the Fermi–Hubbard model, Luther–Emery [4] and FFLO [5] phases are predicted to be observable for ultracold fermions with attractive interaction. In particular, it is well known that

---

[1] Author to whom any correspondence should be addressed.

for the repulsive (positive-U) conventional (Fermi–)Hubbard model the susceptibility for super-fluid and charge-density-wave (CDW) orders are suppressed at low temperatures and the leading quasi-long-range (QLR) order is given by a spin density wave (SDW) at any filling fraction [6].

However, in this work, we show that coexistence of QLR superfluid and CDW orders can be observed for fermionic atoms with repulsive on-site interaction in an anisotropic optical lattice near a wide Feshbach resonance. The interactions in this strongly interacting system can be described by a one-dimensional (1D), positive-U, general Hubbard model (GHM) with particle-assisted tunnelling rates [7]. The GHM is an effective one-band Hamiltonian that takes into account the multi-band populations and the off-site atom–molecule couplings in an optical lattice near a wide Feshbach resonance (see the detailed derivation in [7]). It is interesting to note that the GHM with similar particle-assisted tunnelling also arises in different physical contexts, as proposed in [8]. In contrast to the case of the conventional positive-U Hubbard model, we show that the superfluid and CDW emerge as dominant QLR orders over spin orders for the positive-U GHM when the system is significantly hole-doped below half-filling, although at or very close to half-filling, the dominant correlation in GHM is still anti-ferromagnetic. This feature indicates that the particle-assisted tunnelling in GHM brings in qualitatively new physics. It makes the effective interaction in GHM doping-dependent, showing different behaviours with a possible phase-transition in between. We get our results through numerical calculations based on the time-evolving block-decimation (TEBD) algorithm [9, 10], which, as an extension of the density matrix renormalization group (DMRG) method [11], is a well-controlled approach to deal with 1D systems. We compare our numerical results with some known exact results for the conventional Hubbard model and the remarkably precise agreement shows that the calculation here can make quantitatively reliable predictions.

As shown in [7], a generic Hamiltonian for describing strongly interacting two-component fermions in an optical lattice (or superlattice) is given by the following GHM:

$$H = \sum_i \left[U n_{i\uparrow} n_{i\downarrow} - \mu n_i \right] - \sum_{\langle i,j \rangle, \sigma} \left[t + \delta g \left(n_{i\overline{\sigma}} + n_{j\overline{\sigma}} \right) + \delta t \, n_{i\overline{\sigma}} n_{j\overline{\sigma}} \right] a_{i\sigma}^\dagger a_{j\sigma} + \text{h.c.}, \tag{1}$$

where $n_{i\sigma} \equiv a_{i\sigma}^\dagger a_{i\sigma}$, $n_i \equiv n_{i\uparrow} + n_{i\downarrow}$, μ is the chemical potential, $\langle i, j \rangle$ denotes the neighboring sites and $a_{i\sigma}^\dagger$ is the creation operator for generating a fermion on the site i with the spin index σ. The symbol $\overline{\sigma}$ stands for $(\downarrow, \uparrow)$ for $\sigma = (\uparrow, \downarrow)$. The δg and δt terms in the Hamiltonian represent particle-assisted tunnelling, for which the inter-site tunnelling rate depends on whether there is another atom with opposite spin on these two sites. The particle-assisted tunnelling comes from the multi-band population and the off-site atom–molecule coupling for this strongly interacting system [7]. For atoms near a wide Feshbach resonance with the average filling number $\langle n_i \rangle \leqslant 2$, each lattice site could have four different states, either empty (with state $|0\rangle$), or a spin $\uparrow$ or $\downarrow$ atom ($a_{i\sigma}^\dagger |0\rangle$), or a dressed molecule ($d_i^\dagger |0\rangle$) which is composed of two atoms with opposite spins. The two atoms in a dressed molecule can distribute over a number of lattice bands due to the strong on-site interaction, with the distribution coefficient fixed by solving the single-site problem. One can then mathematically map the dressed molecule state $d_i^\dagger |0\rangle$ to a double-occupation state $a_{i\downarrow}^\dagger a_{i\uparrow}^\dagger |0\rangle$ by using the atomic operators $a_{i\sigma}^\dagger$ [7]. After this mapping, the effective Hamiltonian is transformed to the form of equation (1). The GHM in equation (1) reduces to the conventional Hubbard model when the particle-assisted tunnelling coefficients δg and δt approaching zero, as one moves far away from the Feshbach resonance. Near the resonance, δg and δt can be significant as compared with the atomic tunnelling rate t due to the renormalization from the multi-band populations and the direct neighboring coupling [7].

We consider in this work an anisotropic optical lattice for which the potential barriers along the x- and y-directions are tuned up to completely suppress tunnelling along those directions. The system becomes a set of independent 1D chains. We thus solve the GHM in 1D through numerical analysis. For this purpose, first we transfer all the fermion operators to the hard-core boson operators through the Jordan–Wigner transformation [12]. In the 1D case, we can get rid of the non-local sign factor, and after the transformation the hard-core boson operators satisfy the same Hamiltonian as equation (1). On each site, we then have two hard-core boson modes which are equivalent to a spin-3/2 system with the local Hilbert space dimension $d = 4$. We can therefore use the TEBD algorithm for solving this pseudo-spin system [9]. Similar to the DMRG method [11], the TEBD algorithm is based on the assumption that in the 1D case the ground state $|\Psi\rangle = \sum_{i_1=1}^{d} \cdots \sum_{i_n=1}^{d} c_{i_1\dots i_n} |i_1 \cdots i_n\rangle$ of the Hamiltonian with short-range interactions can be written into the following matrix product form:

$$c_{i_1\dots i_n} = \sum_{\alpha_1,\dots,\alpha_n=1}^{\chi} \Gamma_{\alpha_n\alpha_1}^{[1]i_1} \Gamma_{\alpha_1\alpha_2}^{[2]i_2} \Gamma_{\alpha_2\alpha_3}^{[3]i_2} \cdots \Gamma_{\alpha_{n-1}\alpha_n}^{[n]i_n}, \tag{2}$$

where $\Gamma^{[s]i_s}$ denotes the matrix associated with site-s with the matrix dimension χ. When $\chi = 1$, the assumption reduces to the mean-field approximation, and for a larger χ, the matrix product state well approximates the ground state as it catches the right entanglement structure for 1D systems [9, 10]. To use the TEBD algorithm, we just start with an arbitrary matrix product state in the form of equation (2), and evolve this state with the Hamiltonian (1) in imaginary time through the propagator e^{-Ht}. The state converges to the ground state of the Hamiltonian pretty quickly. From the final ground state in the matrix product form, one can efficiently calculate the reduced density operator and various correlation functions. This calculation has a well-controlled precision since at each time step to update the matrix product state, the Hilbert space truncation error can be suppressed by choosing an appropriate matrix dimension χ [9]. In this calculation, we use the infinite lattice algorithm by assuming that the lattice is bipartite and the ground state has a translational symmetry for each sublattice [9]. This allows us to directly calculate the system in the thermodynamic limit.

To show that our calculation is capable of making reliable predictions, we first test our results by comparing them with some known exact results of the Hubbard model in certain cases. For the Hubbard model at half-filling $\langle n_{i\uparrow}\rangle = \langle n_{i\downarrow}\rangle = 0.5$, the ground state energy per site is known to have the analytic expression $E = -4 \int_0^\infty \frac{J_0(\omega)J_1(\omega)\mathrm{d}\omega}{\omega[1+\exp(\omega U/2)]}$ in the thermodynamic limit from the exact Bethe ansatz solution [13], where J_0 and J_1 are Bessel functions and we have chosen the tunnelling rate t as the energy unit. In figure 1(a), we show our numerical results for the ground state energy of the Hamiltonian (1) with $\delta g = \delta t = 0$, and one can see that it agrees very well with the exact energy of the Hubbard model, in particular when $U > t$. The error is in general smaller than 10^{-3} as shown in figure 1(b). In this and the following calculations, we choose the matrix dimension $\chi = 40$. We have tried larger χ which gives better precision, but we choose $\chi = 40$ to have a faster speed and its precision is enough for our purpose.

We have also tested the final state from our calculation by comparing its correlation functions with some known results. It is difficult to get correlations analytically from the Bethe ansatz solution, but from the bosonization approach to the 1D Hubbard model, we know its correlation functions take certain asymptotic forms. For instance, one can look at the spin–spin correlation, defined as $S_r \equiv \langle s_i \cdot s_{i+r}\rangle$, where the spin operator for the site i is given by $s_i \equiv a_{i\alpha}^\dagger \sigma_{\alpha\beta} a_{i\beta}/2$ with α and $\beta = \downarrow, \uparrow$ and σ standing for the Pauli matrices. The correlation S_r is
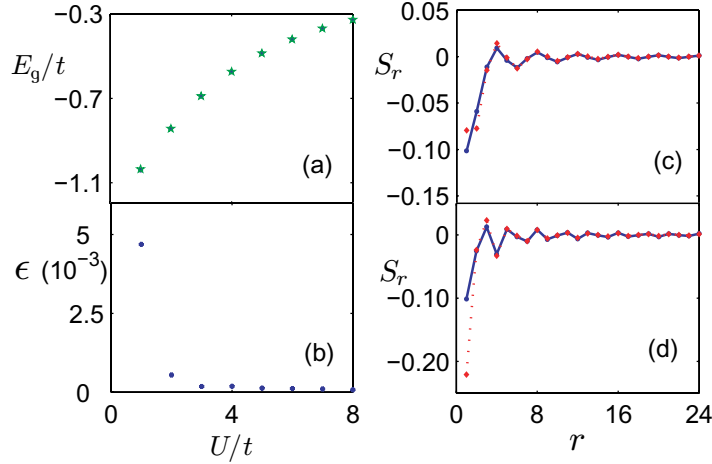
Figure 1. The numerical result for the Hubbard model compared with some known exact results. (a) Ground state energy as a function of U at half-filling (energy in the unit of t), where data points marked by solid dots are from the exact Bethe ansatz solution, while those marked by pentagrams are from our numerical program; (b) the relative error in the ground state energy; (c) real-space spin correlation function at the filling fraction $\langle n_i \rangle = 0.5$ and $U = 8t$, compared with the asymptotic form in equation (3) (solid curve) with $K_\rho = 0.62$ and $A = 0.13$. (d) Similar to (c), except that $\langle n_i \rangle = 0.75$, and the corresponding $K_\rho = 0.60$ and $A = 0.19$.

independent of i because of the translational symmetry. The Hubbard spin correlation function has the following asymptotic form [14]:

$$S_r = -\frac{1}{(\pi r)^2} + \frac{A}{r^{1+K_\rho}} \cos(2k_F r) \ln^{1/2}(r) + \cdots, \tag{3}$$

where K_ρ is the Luttinger parameter whose value has been determined before from the exact Bethe ansatz solution [14, 15], k_F is the fermi momentum related to the filling number $\langle n_i \rangle$ through $k_F = \langle n_i \rangle \pi / 2$, and A is a non-universal model-dependent constant. In figure 1(c) and (d), we compare our calculation results for S_r with this asymptotic form for filling number $\langle n_i \rangle = 0.5$ and 0.75, and the agreement is again remarkable as long as r is not too small (the expression of S_r in equation (3) is not accurate for small r).

With the confidence in numerics built from the above comparison, we now present our main calculation results for the repulsive GHM in equation (1) with $U > 0$. Apart from the spin correlation S_r defined before, we also calculate the CDW correlation, defined as $D_r \equiv \langle n_i n_{i+r} \rangle - \langle n_i \rangle \langle n_{i+r} \rangle$, and the pair (superfluid) correlation, defined as $P_r \equiv \langle a_{i\uparrow} a_{i\downarrow} a_{i+r\downarrow}^\dagger a_{i+r\uparrow}^\dagger \rangle$. The results are shown in figure 2 for different filling fraction $\langle n_i \rangle$ and for models with different particle-assisted tunnelling rates δg and δt. First at half-filling with $\langle n_i \rangle = 1$, the correlation functions S_r, D_r and P_r for the GHM with different δg and δt, all look qualitatively similar to the corresponding results for the conventional Hubbard model, although with increase of the coefficient δg the spin correlation reduces a bit, while the CDW and superfluid correlations increase slightly. Clearly, the dominant correlation in this case is in spin which suggests a QLR anti-ferromagnetic order. In this and the following calculations, we take $U = 8t$ for all the cases, which corresponds to a significant on-site repulsion.
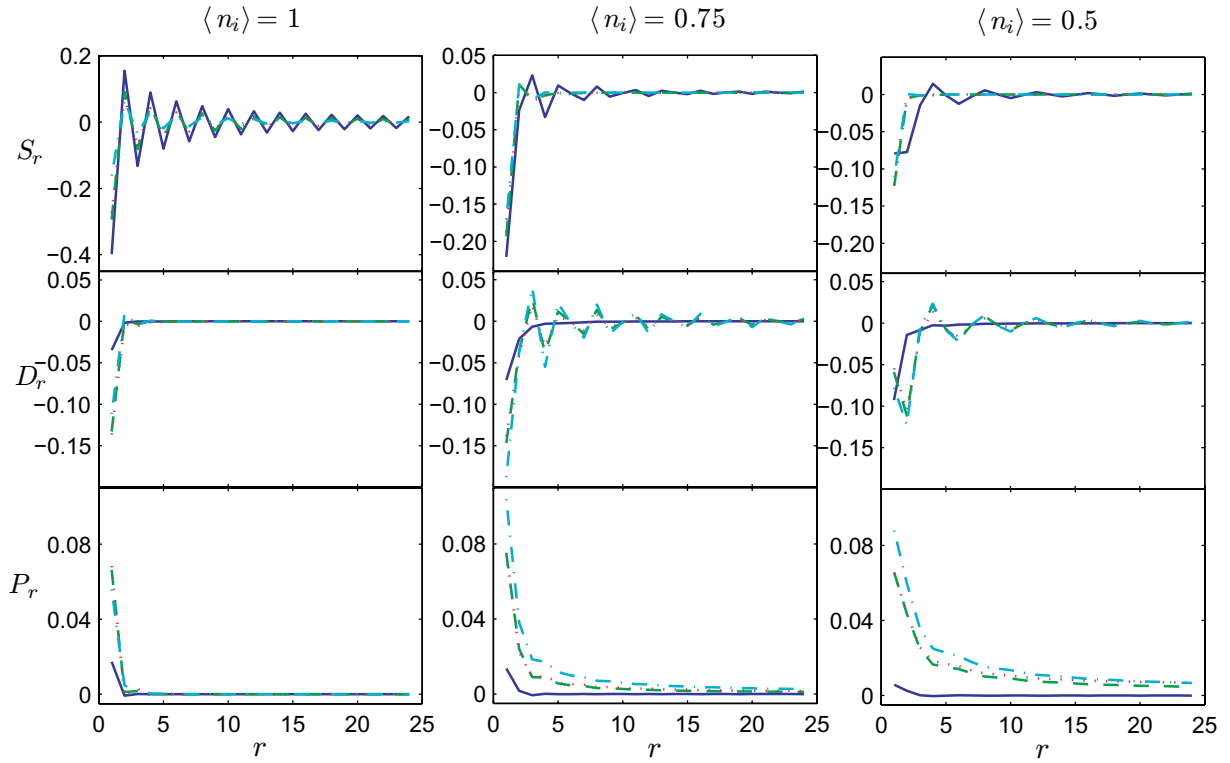
Figure 2. The numerical results for the spin (S_r), the CDW (D_r) and the pair (P_r) correlation functions for the GHM with different particle-assisted tunnelling rates and at different filling fractions, where $\delta g = 0$, $\delta t = 0$ for solid curves, $\delta g = 3t$, $\delta t = -6t$ for dashed curves, $\delta g = 3t$, $\delta t = -3t$ for dotted curves and $\delta g = 7t$, $\delta t = -14t$ for dashed–dotted curves.

Qualitatively different results show up when the system is doped with holes. At the filling fraction $\langle n_i \rangle = 0.75$, although for the Hubbard model the spin correlation is still the dominant one (the SDW order has been pinned to the corresponding $2k_F = 3\pi/4$), for the GHM with a noticeable δg, the superfluid and the CDW emerge as the leading QLR orders, and their correlations increase significantly and decay much slower in space compared with the spin correlation when δg grows. These features become more evident when we further increase the doping. For instance, in the right column of figure 2, we show the correlations for the filling fraction $\langle n_i \rangle = 0.5$. The qualitative behavior is similar to the case with $\langle n_i \rangle = 0.75$, but the CDW and superfluid correlations for the GHM get significantly larger at long distance, and the contrast with the Hubbard model becomes sharper. One can also note that for all these calculations, change of the coefficient δt in the GHM makes little difference to the result. This is understandable as a significant positive-U suppresses the possibility of double occupation in the lattice, and the δt term in the GHM has no effect without double occupation. The δg term in the GHM, however, is critically important, which favors superfluidity in general and brings in the qualitatively different features mentioned above.

To show the spatial structure of these QLR orders, we plot in figure 3 the spin, the CDW and superfluid correlations in the momentum space for the GHM with $\delta g = 3t$ at different filling fractions $\langle n_i \rangle$. The momentum space correlations are defined by the Fourier transform
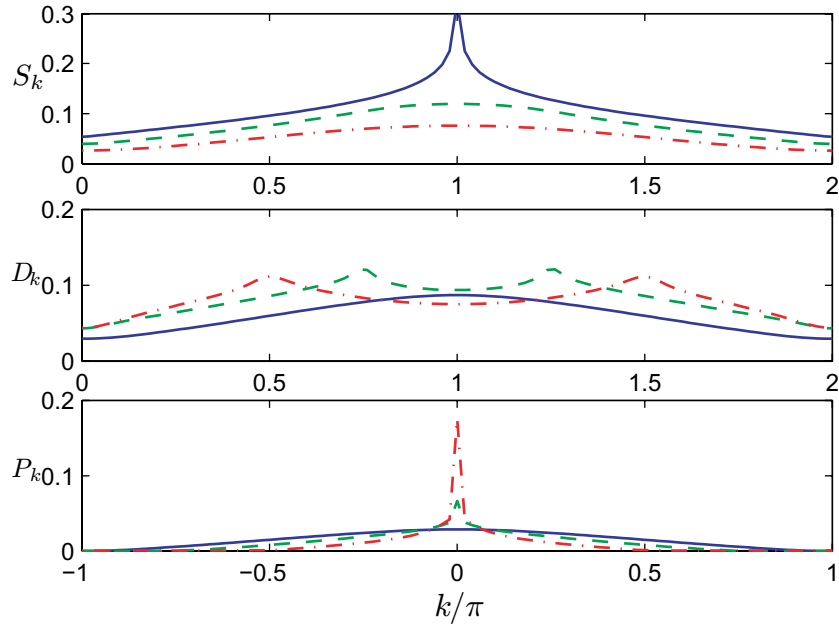
Figure 3. The spin, the CDW and the pair correlation functions in momentum space for the GHM with $\delta g = 3t$ and $\delta t = -3t$. The solid, dashed and dashed–dotted curves correspond to filling factor $\langle n_i \rangle = 1$, 0.75 and 0.5, respectively. For the calculation of the Fourier transformation, we have used the real space correlation functions for $N = 100$ sites.

$X_k = 1/\sqrt{N} \sum_{r=0}^{N} X_r \cos(kr)$, where X stands for the correlations S, D, or P. From these momentum space curves, one can clearly see that this GHM at half-filling has a QLR anti-ferromagnetic order (characterized by the peak at $k = \pi$), and away from half-filling a QLR superfluid order (peak at $k = 0$) and CDW order (peaks at $k = 2k_F$ and $2\pi - 2k_F$, where $2k_F = 3\pi/4$ ($\pi/2$) for the filling fractions $\langle n_i \rangle = 0.75$ (0.5), respectively. The peaks in figure 3 have finite widths because these orders in 1D are only QLR with algebraic decay. Note that if we turn on small tunnelling interaction between different 1D chains, a leading QLR order, such as superfluid order, could be stabilized to a true long-range order [6]. The GHM thus provides an example of a microscopic Hamiltonian that with hole doping from half-filling, an anti-ferromagnetic phase could be transferred to a superfluid phase (or a CDW phase in some cases depending on which order becomes more dominant with the inter-chain coupling). The correlations that characterize these QLR orders can be detected for the cold atomic gas, for instance, through the method described in [16].

In summary, we have investigated the ground state properties of the GHM with repulsive on-site interaction in 1D through well-controlled numerical analysis. For the system with significant particle-assisted tunnelling rates δg and δt, we have found coexistence of QLR superfluid and CDW orders when the system is hole-doped from half-filling. This feature is in sharp contrast with the conventional Hubbard model, in which case for positive-U the charge and superfluid orders are always suppressed regardless of the filling fraction. With a combination of the Bosonization approach and the TEBD or DMRG numerical algorithm, it may be possible to determine the complete phase diagram for GHM. The model here describes strongly interacting fermionic atoms in an anisotropic optical lattice. The possibility of a transition from

an anti-ferromagnetic phase to a superfluid phase for the GHM with hole-doping may also have interesting indications for other areas.

Acknowledgments

References

[1] Chin J K *et al* 2006 *Nature* **443** 961
    Stoferle T *et al* 2006 *Phys. Rev. Lett.* **96** 030401
[2] Jaksch D, Bruder C, Cirac J I, Gardiner C W and Zoller P 1998 *Phys. Rev. Lett.* **81** 3108
[3] Scarola V W, Demler E and Das Sarma S 2006 *Phys. Rev.* A **73** 051601
[4] Gao X-L *et al* 2007 *Phys. Rev. Lett.* **98** 030404
    Pour F K *et al* 2007 *Phys. Rev.* B **75** 161104
[5] Feiguin A and Heidrich-Meisner F 2007 *Phys. Rev.* B **76** 220508
[6] Carlson E W, Emery V J, Kivelson S A and Orgad D 2003 *The Physics of Superconductors* (Berlin: Springer)
    pp 275–452 (*Preprint* cond-mat/0206217)
[7] Duan L M 2005 *Phys. Rev. Lett.* **95** 243202
    Duan L M 2007 *Preprint* 0706.2161
[8] Hirsch J E 1989 *Physica* C **158** 326
    Strack R and Vollhardt D 1993 *Phys. Rev. Lett.* **70** 2637
    Arrachea L and Aligia A A 1994 *Phys. Rev. Lett.* **73** 2240
[9] Vidal G 2004 *Phys. Rev. Lett.* **93** 040502
    White S R and Feiguin A E 2004 *Phys. Rev. Lett.* **93** 076401
    Daley A J *et al* 2004 *J. Stat. Mech.: Theor. Exp.* P04005
    Verstraete F and Cirac J I 2006 *Preprint* cond-mat/0407066
    Shi Y Y, Duan L M and Vidal G 2006 *Phys. Rev.* A **74** 022320
[10] Vidal G 2007 *Phys. Rev. Lett.* **98** 070201
[11] White S R 1992 *Phys. Rev. Lett.* **69** 2863
[12] Jordan P and Wigner E 1928 *Z. Phys.* **47** 631
[13] Lieb E H and Wu F Y 1968 *Phys. Rev. Lett.* **20** 1445
[14] Schulz H J 1991 *Int. J. Mod. Phys.* B **5** 57
[15] Schulz H J 1990 *Phys. Rev. Lett.* **64** 2831
[16] Duan L-M 2006 *Phys. Rev. Lett.* **96** 103201